

*Proceedings of the 9th International Conference on
Applied Operational Research (ICAOR 2017)
Chung Yuan Christian University
Taoyuan, Taiwan
18-20 December 2017*

Simulated annealing optimization of tuned mass dampers for vibration control of seismic-excited buildings

Ming-Yi Liu ^{1,*}, Wen-Che Liang ² and Yun-Zhu Lin ¹

¹ Department of Civil Engineering, Chung Yuan Christian University, Taoyuan City, Taiwan

² Department of Civil Engineering, National Cheng Kung University, Tainan City, Taiwan

Abstract

The objective of this paper is to investigate the simulated annealing optimization of tuned mass dampers (TMDs) for vibration control of high-rise buildings under seismic excitations. The computational procedure for an analytical model, including the frequency domain analysis, optimization analysis and time domain analysis, is presented for this purpose. Numerical examples, including the model validation and effectiveness assessment, are also provided to illustrate the analytical model. The numerical results determined by the simulated annealing are consistent with the exact solutions obtained from the gradient-based algorithm, suggesting that the simulated annealing provides the sufficient accuracy for such problems. Furthermore, the dynamic displacements of the main structure can be successfully controlled by the TMD, indicating that the vibration energy transferred from the main structure to the TMD is attributed to the frequency loci veering and mode localization when the natural frequency of the main structure and that of the TMD approach one another.

Keywords: simulated annealing optimization; tuned mass damper; seismic-excited building; vibration control

Introduction

In the last several decades, light-weight and high-strength materials have been widely used in the construction of high-rise buildings. Such structures are susceptible to seismic excitations due to their light, flexible and low-damping characteristics. Under these conditions, large-amplitude vibrations of high-rise buildings during strong earthquakes greatly affect the structural safety, which is a significant concern for design purposes. Consequently, a variety of passive energy dissipation devices installed in high-rise buildings have been extensively applied to reduce structural responses (Soong and Dargush 1997). Among these devices, a tuned mass damper (TMD) consisting of a mass-spring-dashpot system is the first one to be theoretically studied from the academic viewpoint (Frahm 1911). For the engineering applications, TMDs have been successfully realized for vibration control of high-rise buildings, such as the John Hancock Tower in Boston, the Citigroup Center in New York City and the Taipei 101 in Taipei (Taranath 2005).

A two-mass system consisting of a TMD attached to a main structure idealized as a single-degree-of-freedom (SDOF) system under excitations can be used to explain the energy dissipation mechanism of the damper. The vibration of the main structure causes the TMD to vibrate in resonance when the natural frequency of the TMD is tuned to be close to that of the main structure, resulting in the fact that a large amount of vibration energy of the main structure is transferred to the TMD and then dissipated by the damping of the TMD. To achieve the best control performance, a variety of optimization criteria expressed as objective functions have been proposed to determine the TMD

* *Correspondence:* Ming-Yi Liu

Department of Civil Engineering, Chung Yuan Christian University, No. 200, Chung Pei Road, Chungli District, Taoyuan City 32023, Taiwan
myliu@cycu.edu.tw

parameters, including the tuning frequency and damping ratios. Based on gradient-based algorithms, the optimal TMD parameters can be obtained by either maximizing or minimizing the objective functions. In consideration of the optimization criteria to minimize the dynamic responses of the main structure subjected to either external forces or base accelerations, four types of analytical models: a TMD attached to an undamped SDOF system under harmonic excitations (Den Hartog 1956; Neubert 1964; Warburton 1982), a TMD attached to an undamped SDOF system under white noise excitations (Ayorinde and Warburton 1980; Warburton 1982), a TMD attached to a damped SDOF system under harmonic excitations (Warburton and Ayorinde 1980) and a TMD attached to a damped SDOF system under white noise excitations (Warburton 1982), have been presented to determine the optimal TMD parameters. For the undamped SDOF system under either harmonic or white noise excitations, the optimal tuning frequency and damping ratios are both explicitly formulated in terms of the mass ratio. The explicit formulas for the two optimal TMD parameters, however, no longer exist for the damped SDOF system under either harmonic or white noise excitations. Under these conditions, numerical iteration schemes are used to obtain both the optimal tuning frequency and damping ratios for a given mass ratio.

In the studies mentioned above, the optimization of TMD parameters with relatively simple objective functions can only be applicable to simplified SDOF systems for both harmonic and white noise excitations. Such limitations have to be eliminated to more appropriately capture the complex characteristics of real high-rise buildings under seismic excitations. Under these conditions, however, the objective functions tend to be discontinuous, nondifferentiable, stochastic, and/or highly nonlinear, implying that it is difficult to determine the optimal TMD parameters by gradient-based algorithms.

To overcome the limitations of gradient-based algorithms, metaheuristic algorithms inspired by natural phenomena, including the genetic algorithm (Hadi and Arfiadi 1998; Mohebbi and Joghataie 2012), particle swarm optimization (Leung et al. 2008; Leung and Zhang 2009), harmony search (Bekdaş and Nigdeli 2011) and ant colony optimization (Farshidianfar and Soheili 2013), have been rapidly applied to solve TMD optimization problems. Unlike the gradient-based algorithms, the metaheuristic algorithms are without restrictions on the derivative information about objective functions, and the corresponding optimal TMD parameters can then be obtained for an appropriate balance between the global exploration and local search abilities (Yang 2010).

The simulated annealing categorized as metaheuristic algorithms was first proposed to solve traveling salesman problems (Kirkpatrick et al. 1983). This type of algorithm inspired by the annealing process of metals involves the heating and cooling stages for the purpose of increasing the size of the metal crystals as well as reducing their defects. In the heating stage, the metals are initially heated to a high temperature that allows the metal particles to move freely with respect to each other, while in the cooling stage, the metal particles rearrange into a crystalline state with the minimum energy when the metal temperature decreases for a specific cooling rate. The simulated annealing has been successfully applied to many engineering fields (Siddique and Adeli 2016), however, few applications have been devoted to TMD optimization problems.

The objective of this paper is to investigate the simulated annealing optimization of TMDs for vibration control of high-rise buildings under seismic excitations. The computational procedure for an analytical model is presented for this purpose. Numerical examples are also provided to illustrate the analytical model.

Analytical model

The computational procedure for an analytical model, including the frequency domain analysis, optimization analysis and time domain analysis, is presented in this study, which will be discussed in this section.

The frequency domain analysis is conducted to calculate the dynamic responses of seismic-excited buildings using the random vibration theory (Crandall and Mark 1963). For this purpose, based on the previous literature (Warburton 1982), the analytical model for a two-mass system consisting of a TMD attached to a damped main structure subjected to base accelerations is illustrated in Figure 1, where M , K , C and $X(t)$ are the mass, stiffness, damping and displacement time history relative to the base of the main structure, respectively, and t is the time; M_D , K_D , C_D and

$X_D(t)$ are the mass, stiffness, damping and displacement time history relative to the base of the TMD, respectively; $X_G(t)$ and $\ddot{X}_G(t)$ are the displacement and acceleration time histories of the base, respectively. To facilitate an improved understanding of the dynamics of the two-mass system, one introduces a number of significant parameters: the natural frequency of the main structure $\omega = \sqrt{K/M}$, damping ratio of the main structure $\zeta = C/2\sqrt{KM}$, natural frequency of the TMD $\omega_D = \sqrt{K_D/M_D}$, damping ratio of the TMD $\zeta_D = C_D/2\sqrt{K_D M_D}$, mass ratio $\mu = M_D/M$ and tuning frequency ratio $f = \omega_D/\omega$. Furthermore, the base accelerations induced by earthquakes are assumed to be white noise excitations with a constant spectral density S_0 . Based on the above mentioned parameters, one can derive the equations of motion for the analytical model, and then determine the corresponding nondimensional complex frequency response function and variance of displacement of the main structure relative to the base, denoted $H(r)$ and N , respectively, where r is the excitation frequency ratio.

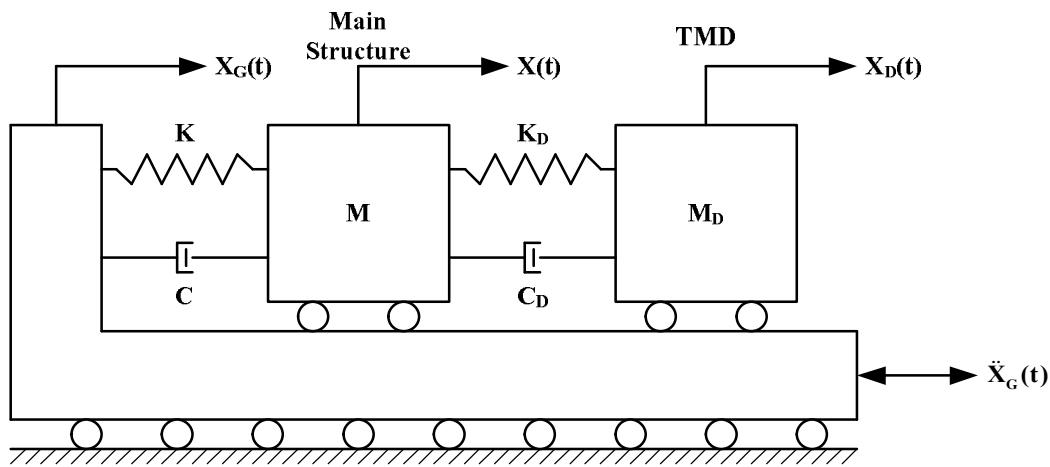


Figure 1. Analytical model for two-mass system subjected to base accelerations.

The optimization analysis is conducted to determine the optimal TMD parameters for vibration control of seismic-excited buildings using the simulated annealing (Kirkpatrick et al. 1983). Based on the results of the frequency domain analysis, the optimal values of f and ζ_D , denoted f^{opt} and ζ_D^{opt} , respectively, can be obtained by minimizing N as the objective function value N^{min} for given values of μ and ζ . The simulated annealing algorithm is summarized in the following procedure:

1. *Define the problem.* Determine the objective function $f(x)$, the design point $x = (x_1, x_2, \dots, x_n)^T$, the l th design variable x_l ($l=1,2,\dots,n$), the number of design variables n , the initial design point $x^{(0)}$ and the initial objective function value $f(x^{(0)})$.
2. *Select the annealing schedule parameters.* Determine the initial temperature T_0 , the final temperature T_f , the cooling factor $\alpha \in (0, 1)$ and the maximum number of cooling stages n_c , and initialize the outer loop counter $i = 0$.
3. *Select the iteration parameters.* Determine the maximum number of iterations n_i and initialize the inner loop counter $j = 1$.
4. *Perform the annealing schedule.* Calculate the i th cooling temperature ($i = 0,1,2,\dots,n_c$)

$$T^{(i)} = T_0 \alpha^i, \quad (1)$$

where $T^{(i)} = T_0$ for $i = 0$ and $T^{(i)} = T_f$ for $i = n_c$.

5. *Perform the iteration.* Calculate the j th iteration design point ($j = 1, 2, \dots, n_i$)

$$x^{(j)} = x^{(j-1)} + r, \quad (2)$$

and the difference between the corresponding objective function values

$$\Delta f = f(x^{(j)}) - f(x^{(j-1)}), \quad (3)$$

where r is the random number. If $\Delta f < 0$, then accept $x^{(j)}$ and $f(x^{(j)})$ as the better design point and objective function value, respectively; go to step 6. If $\Delta f \geq 0$, then calculate the Boltzmann probability density function value

$$p(\Delta f) = e^{-\frac{\Delta f}{T^{(j)}}}, \quad (4)$$

and generate the uniform random number $u \in [0, 1]$. If $p(\Delta f) > u$, then accept $x^{(j)}$ and $f(x^{(j)})$ as the better design point and objective function value, respectively; go to step 6. If $p(\Delta f) \leq u$, then repeat step 5.

6. *Update the inner loop counter.* If $j < n_i$, then set $j = j + 1$; return to step 5. If $j = n_i$, then let $x^{(0)} = x^{(j)}$ and $f(x^{(0)}) = f(x^{(j)})$; set $j = 1$; go to step 7.

7. *Update the outer loop counter.* If $i < n_c$, then set $i = i + 1$; return to step 4. If $i = n_c$, then determine $x^{(j)}$ and $f(x^{(j)})$ as the optimal design point and objective function value, respectively.

The time domain analysis is conducted to assess the effectiveness of TMDs for vibration control of seismic-excited buildings using the linear acceleration method (Newmark 1959). Based on f^{opt} and ζ_D^{opt} obtained from the optimization analysis, $X(t)$ as well as the corresponding root-mean-square (RMS) and peak values for two types of systems: with and without damper, can be calculated according to the equations of motion for each system under seismic excitations. Under these conditions, the effectiveness of the TMD can be quantitatively assessed by comparing the response reduction rates between the two systems.

Numerical examples

In order to illustrate the computational procedure for the analytical model in this study, numerical examples, including the model validation and effectiveness assessment, are provided and discussed in this section.

The model validation is conducted to evaluate the accuracy of the simulated annealing applied to TMD optimization problems for vibration control of seismic-excited buildings. For this purpose, based on the analytical model in Figure 1, the optimal TMD parameters determined by the simulated annealing are compared with values obtained from the gradient-based algorithm presented in the previous literature (Warburton 1982). In this study, the annealing schedule parameters are selected as $T_0 = 10^3$ °C, $T_f = 10^{-5}$ °C and $\alpha = 0.9$. Figures 2 to 4 show the variations of f^{opt} , ζ_D^{opt} and N^{min} with μ for various values of ζ , corresponding to the simulated annealing and gradient-based algorithm, respectively. These three figures illustrate that both f^{opt} and N^{min} decrease monotonically, while ζ_D^{opt} increases monotonically with increasing μ or ζ . Consequently, under the conditions of the two-mass system with a larger mass ratio or higher inherent damping ratio, the TMD, accompanied by a lower optimal tuning frequency ratio and higher optimal damping ratio, can be used to more effectively suppress the variance of displacements of the main structure subjected to base accelerations simulated by white noise excitations. Furthermore, the numerical results determined by the simulated annealing are consistent with the exact solutions obtained from the gradient-based algorithm, suggesting that the simulated annealing provides the sufficient accuracy for such problems.

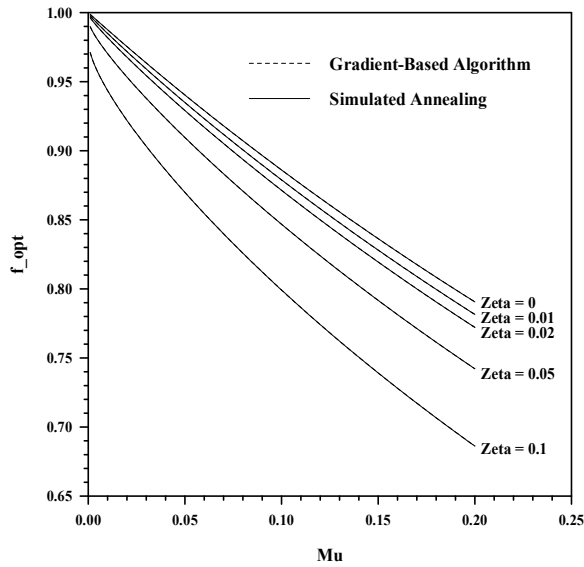


Figure 2. Variation of optimal tuning frequency ratio with mass ratio.

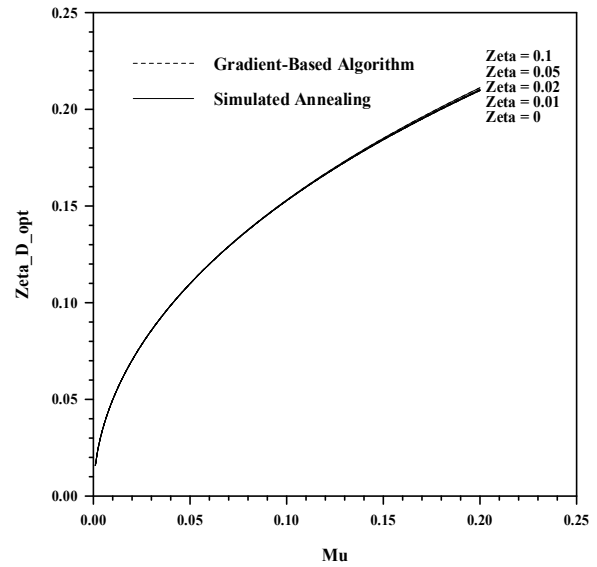


Figure 3. Variation of optimal TMD damping ratio with mass ratio.

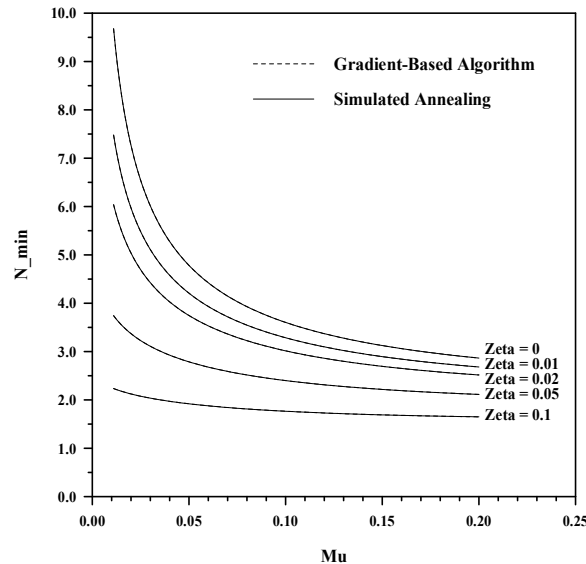


Figure 4. Variation of minimum objective function value with mass ratio.

The effectiveness assessment is conducted to assess the effectiveness of TMDs for vibration control of seismic-excited buildings. Based on the simulated annealing with sufficient accuracy verified by the model validation, real cases of the TMD installed in the Taipei 101 subjected to a variety of seismic ground accelerations are studied for this purpose. In order to apply the two-mass system to such real cases, the Taipei 101 is simplified to a damped SDOF system with $M = 8.46 \times 10^7$ kg, $K = 7.12 \times 10^7$ N/m, $C = 1.55 \times 10^6$ N-s/m, $\omega = 0.9174$ rad/s and $\zeta = 0.0100$, the pendulum-type TMD is considered to be equivalent to a mass-spring-dashpot system with $M_D = 6.60 \times 10^5$ kg, and $\mu = M_D/M = 0.0078$ is then calculated (Zuo and Cui 2013). Under these conditions, $f^{opt} = 0.9879$ and $\zeta_D^{opt} = 0.0441$ are determined by the simulated annealing, and $K_D = 5.42 \times 10^5$ N/m, $C_D = 5.27 \times 10^4$ N-s/m and $\omega_D = 0.9063$ rad/s are then calculated from the formulas in the previous section. In order to increase the generality of the effectiveness assessment results, forty-two seismic ground accelerations induced by twenty-one earthquakes are selected from the NGA-West2 database developed by the Pacific Earthquake Engineering Research Center at the University of California, Berkeley (Ancheta et

al. 2014), as summarized in Table 1. Based on the above mentioned parameters, the dynamic displacements of the Taipei 101 subjected to the seismic ground accelerations are calculated using the linear acceleration method, as listed in Table 2. These data reveal that among the total of forty-two cases, the RMS response reduction rates are between 1.0141% and 36.8384%, while the peak values are between 0.0116% and 19.8985%. Furthermore, for each of the thirty-four cases, the RMS response reduction rate is higher than the peak value. Consequently, compared to the peak displacements, the TMD can be used to more effectively suppress the RMS displacements of the main structure subjected to real seismic ground accelerations in most cases.

Table 1. Seismic ground accelerations selected from the NGA-West2 database (Ancheta et al. 2014).

Number	Date	Location	Magnitude	Seismic Station	Horizontal Component 1	Horizontal Component 2	PGA (g)*
1	1971/02/09	San Fernando, CA, USA	6.6	LA – Hollywood Stor	SFERN/PEL090	SFERN/PEL180	0.21
2	1976/05/06	Friuli, Italy	6.5	Tolmezzo	FRIULLA/A-TMZ000	FRIULLA/A-TMZ270	0.35
3	1979/10/15	Imperial Valley, CA, USA	6.5	Delta	IMPVALL.H/H-DLT262	IMPVALL.H/H-DLT352	0.35
4	1979/10/15	Imperial Valley, CA, USA	6.5	El Centro Array #11	IMPVALL.H/H-E11140	IMPVALL.H/H-E11230	0.38
5	1987/11/24	Superstition Hills, CA, USA	6.5	El Centro Imp. Co.	SUPER.B/B-ICC000	SUPER.B/B-ICC090	0.36
6	1987/11/24	Superstition Hills, CA, USA	6.5	Poe Road (temp)	SUPER.B/B-POE270	SUPER.B/B-POE360	0.45
7	1989/10/18	Loma Prieta, CA, USA	6.9	Capitola	LOMAP/CAP000	LOMAP/CAP090	0.53
8	1989/10/18	Loma Prieta, CA, USA	6.9	Gilroy Array #3	LOMAP/G03000	LOMAP/G03090	0.56
9	1992/06/28	Landers, CA, USA	7.3	Coolwater	LANDERS/CLW-LN	LANDERS/CLW-TR	0.42
10	1992/06/28	Landers, CA, USA	7.3	Yermo Fire Station	LANDERS/YER270	LANDERS/YER360	0.24
11	1994/01/17	Northridge, CA, USA	6.7	Beverly Hills – 14145 Mudhol	NORTHR/MUL009	NORTHR/MUL279	0.52
12	1994/01/17	Northridge, CA, USA	6.7	Canyon Country – W Lost Cany	NORTHR/LOS000	NORTHR/LOS270	0.48
13	1995/01/16	Kobe, Japan	6.9	Nishi-Akashi	KOBE/NIS000	KOBE/NIS090	0.51
14	1995/01/16	Kobe, Japan	6.9	Shin-Osaka	KOBE/SHI000	KOBE/SHI090	0.24
15	1999/08/17	Kocaeli, Turkey	7.5	Arcecik	KOCAELI/ARE000	KOCAELI/ARE090	0.22
16	1999/08/17	Kocaeli, Turkey	7.5	Duzce	KOCAELI/DZC180	KOCAELI/DZC270	0.36
17	1999/09/20	Chi-Chi, Taiwan	7.6	CHY101	CHICHI/CHY101-E	CHICHI/CHY101-N	0.44
18	1999/09/20	Chi-Chi, Taiwan	7.6	TCU045	CHICHI/TCU045-E	CHICHI/TCU045-N	0.51
19	1999/11/12	Duzce, Turkey	7.1	Bolu	DUZCE/BOL000	DUZCE/BOL090	0.82
20	1990/06/20	Manjil, Iran	7.4	Abbar	MANJIL/ABBAR--L	MANJIL/ABBAR--T	0.51
21	1999/10/16	Hector Mine, CA, USA	7.1	Hector	HECTOR/HEC000	HECTOR/HEC090	0.34

* The larger value of the two components is listed.

Table 2. Dynamic displacements of the Taipei 101 subjected to seismic ground accelerations selected from the NGA-West2 database.

Number	Horizontal Component 1						Horizontal Component 2					
	RMS Displacement (m)		Response Reduction Rate (%)	Peak Displacement (m)		Response Reduction Rate (%)	RMS Displacement (m)		Response Reduction Rate (%)	Peak Displacement (m)		Response Reduction Rate (%)
	Without TMD	With TMD		Without TMD	With TMD		Without TMD	With TMD		Without TMD	With TMD	
1	0.1057	0.0743	29.6816	0.3223	0.3195	0.8662	0.1289	0.0814	36.8384	0.2360	0.2321	1.6808
2	0.0435	0.0363	16.6685	0.0766	0.0765	0.2030	0.0412	0.0358	13.0437	0.0941	0.0933	0.8566
3	0.2325	0.1646	29.2051	0.5716	0.4578	19.8985	0.2076	0.1720	17.1182	0.5093	0.4205	17.4246
4	0.3578	0.3198	10.6370	0.7596	0.6188	18.5259	0.5379	0.4565	15.1439	1.0130	0.8793	13.2032
5	0.4610	0.4184	9.2437	1.2046	1.0980	8.8482	0.5199	0.4679	9.9883	1.3828	1.2389	10.4078
6	0.0512	0.0503	1.7652	0.1153	0.1151	0.1877	0.1625	0.1571	3.3262	0.4131	0.3938	4.6597
7	0.0334	0.0289	13.4897	0.0784	0.0761	2.8636	0.0184	0.0181	1.6993	0.0607	0.0606	0.1385
8	0.1265	0.1035	18.1667	0.2406	0.2138	11.1704	0.0895	0.0809	9.5491	0.2495	0.2486	0.3503
9	0.2081	0.2028	2.5113	0.5285	0.5188	1.8386	0.2201	0.2118	3.7641	0.5623	0.5437	3.2971
10	0.5506	0.4794	12.9421	1.1851	1.1377	3.9953	0.3008	0.2678	10.9726	0.5981	0.5980	0.0116
11	0.0548	0.0523	4.5436	0.2099	0.2098	0.0824	0.0587	0.0529	9.9697	0.2304	0.2288	0.6956
12	0.0478	0.0469	1.9003	0.1591	0.1589	0.1006	0.1086	0.1037	4.5185	0.2043	0.1863	8.8130
13	0.0977	0.0807	17.4358	0.1702	0.1599	6.0504	0.1998	0.1667	16.5703	0.3967	0.3875	2.3181
14	0.0490	0.0450	8.2192	0.1137	0.1130	0.6518	0.0931	0.0814	12.5572	0.2097	0.1897	9.5485
15	0.1259	0.1204	4.3793	0.2838	0.2813	0.8808	0.4228	0.4017	5.0026	0.9075	0.9017	0.6416
16	0.7087	0.6647	6.2084	1.5456	1.3785	10.8111	0.3360	0.3142	6.4834	0.6452	0.5981	7.2980
17	0.5543	0.3951	28.7129	1.2081	1.1854	1.8807	0.9253	0.7221	21.9602	2.5089	2.4291	3.1836
18	0.4482	0.3392	24.3158	1.0133	0.9583	5.4287	0.2175	0.1567	27.9568	0.4912	0.4235	13.7670
19	0.2708	0.2091	22.7948	0.5476	0.5383	1.6854	0.1524	0.1112	27.0236	0.2985	0.2787	6.6280
20	0.2320	0.2296	1.0141	0.4563	0.4350	4.6637	0.4530	0.3718	17.9246	0.8049	0.7224	10.2504
21	0.2464	0.2001	18.8106	0.4316	0.4061	5.9036	0.1467	0.1194	18.6078	0.2976	0.2795	6.0741

To extend the results of Tables 1 and 2, under the excitation of the horizontal component 2 of the San Fernando earthquake accelerogram recorded on February 9, 1971 in Figure 5, the displacement time histories of the Taipei 101 and its TMD are provided in Figure 6. These curves illustrate that $X(t)$ with TMD is relatively lower than that without TMD, and $X_D(t)$ is significantly higher than $X(t)$ with TMD. Consequently, the dynamic displacements of the main structure can be successfully controlled by the TMD, indicating that the vibration energy transferred from the main structure to the TMD is attributed to the frequency loci veering and mode localization when the natural frequency of the main structure and that of the TMD approach one another. A more detailed description of such mechanism can be found in the authors' previous work (Liu et al. 2013).

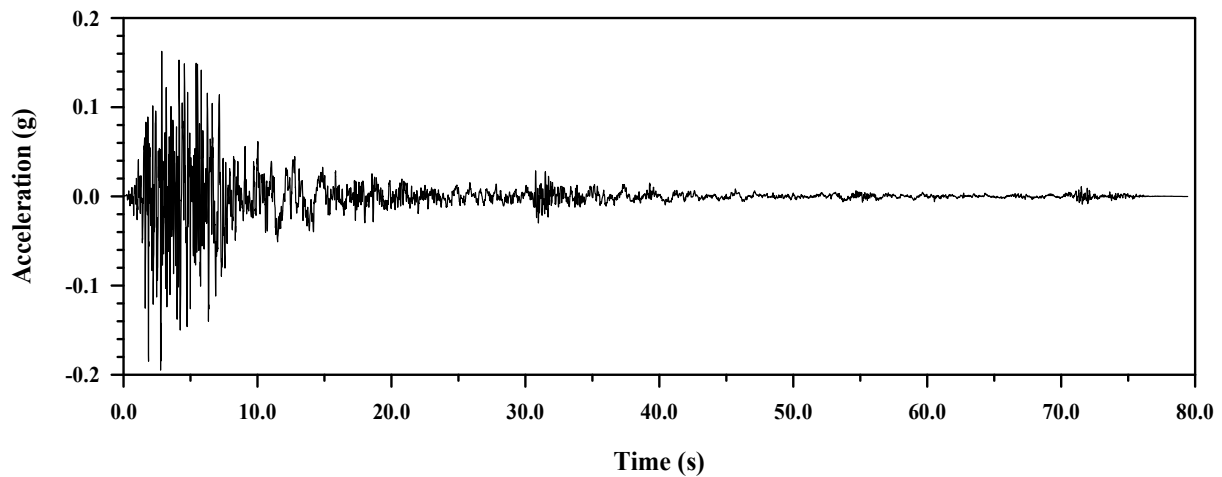


Figure 5. Horizontal component 2 of the San Fernando earthquake accelerogram (Ancheta et al. 2014).

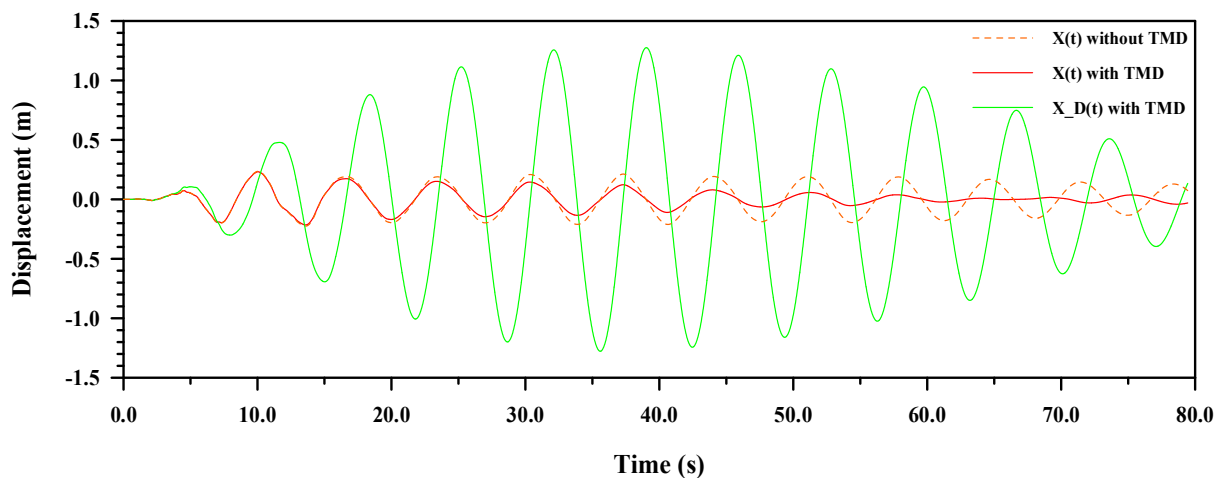


Figure 6. Displacement time histories of the Taipei 101 and its TMD subjected to horizontal component 2 of the San Fernando earthquake accelerogram.

Conclusions

The objective of this paper is to investigate the simulated annealing optimization of TMDs for vibration control of high-rise buildings under seismic excitations. The computational procedure for an analytical model, including the frequency domain analysis, optimization analysis and time domain analysis, is presented for this purpose. Numerical examples, including the model validation and effectiveness assessment, are also provided to illustrate the analytical model. A number of conclusions can be drawn from this study:

1. The numerical results determined by the simulated annealing are consistent with the exact solutions obtained from the gradient-based algorithm, suggesting that the simulated annealing provides the sufficient accuracy for such problems.
2. Under the conditions of the two-mass system with a larger mass ratio or higher inherent damping ratio, the TMD, accompanied by a lower optimal tuning frequency ratio and higher optimal damping ratio, can be used to more effectively suppress the variance of displacements of the main structure subjected to base accelerations simulated by white noise excitations.
3. Compared to the peak displacements, the TMD can be used to more effectively suppress the RMS displacements of the main structure subjected to real seismic ground accelerations in most cases.
4. The dynamic displacements of the main structure can be successfully controlled by the TMD, indicating that the vibration energy transferred from the main structure to the TMD is attributed to the frequency loci veering and mode localization when the natural frequency of the main structure and that of the TMD approach one another.

References

- Ancheta, T.D., Darragh, R.B., Stewart, J.P., Seyhan, E., Silva, W.J., Chiou, B.S.J., Wooddell, K.E., Graves, R.W., Kottke, A.R., Boore, D.M., Kishida, T., and Donahue, J.L. (2014). "NGA-West2 database." *Earthquake Spectra*, EERI, 30(3), 989-1005.
- Ayorinde, E.O., and Warburton, G.B. (1980). "Minimizing structural vibrations with absorbers." *Earthquake Engineering and Structural Dynamics*, 8(3), 219-236.
- Bekdaş, G., and Nigdeli, S.M. (2011). "Estimating optimum parameters of tuned mass dampers using harmony search." *Engineering Structures*, 33(9), 2716-2723.
- Crandall, S.H., and Mark, W.D. (1963). "Random vibration in mechanical systems." Academic Press, Inc., New York City, New York, USA.
- Den Hartog, J.P. (1956). "Mechanical vibrations." Fourth Edition, McGraw-Hill Book Company, Inc., New York City, New York, USA.
- Farshidianfar, A., and Soheili, S. (2013). "Ant colony optimization of tuned mass dampers for earthquake oscillations of high-rise structures including soil-structure interaction." *Soil Dynamics and Earthquake Engineering*, 51, 14-22.
- Frahm, H. (1911). "Device for damping vibrations of bodies." US Patent 989,958, April 18, 1911.
- Hadi, M.N.S., and Arfiadi, Y. (1998). "Optimum design of absorber for MDOF structures." *Journal of Structural Engineering*, ASCE, 124(11), 1272-1280.
- Kirkpatrick, S., Gelatt Jr., C.D., and Vecchi, M.P. (1983). "Optimization by simulated annealing." *Science*, 220(4598), 671-680.
- Leung, A.Y.T., and Zhang, H. (2009). "Particle swarm optimization of tuned mass dampers." *Engineering Structures*, 31(3), 715-728.
- Leung, A.Y.T., Zhang, H., Cheng, C.C., and Lee, Y.Y. (2008). "Particle swarm optimization of TMD by non-stationary base excitation during earthquake." *Earthquake Engineering and Structural Dynamics*, 37(9), 1223-1246.
- Liu, M.Y., Zuo, D., and Jones, N.P. (2013). "Analytical and numerical study of deck-stay interaction in a cable-stayed bridge in the context of field observations." *Journal of Engineering Mechanics*, ASCE, 139(11), 1636-1652.
- Mohebbi, M., and Joghataie, A. (2012). "Designing optimal tuned mass dampers for nonlinear frames by distributed genetic algorithms." *The Structural Design of Tall and Special Buildings*, 21(1), 57-76.
- Neubert, V.H. (1964). "Dynamic absorbers applied to a bar that has solid damping." *Journal of Acoustical Society of America*, 36(4), 673-680.
- Newmark, N.M. (1959). "A method of computation for structural dynamics." *Journal of Engineering Mechanics Division*, ASCE, 85(EM3), 67-94.
- Siddique, N., and Adeli, H. (2016). "Simulated annealing, its variants and engineering applications." *International Journal on Artificial Intelligence Tools*, 25(6), 1630001-1-1630001-24.
- Soong, T.T., and Dargush, G.F. (1997). "Passive energy dissipation systems in structural engineering." John Wiley & Sons, Ltd., Chichester, UK.

- Taranath, B.S. (2005). "Wind and earthquake resistant buildings: Structural analysis and design." CRC Press, Taylor & Francis Group, LLC, Boca Raton, Florida, USA.
- Warburton, G.B. (1982). "Optimum absorber parameters for various combinations of response and excitation parameters." *Earthquake Engineering and Structural Dynamics*, 10(3), 381-401.
- Warburton, G.B., and Ayorinde, E.O. (1980). "Optimum absorber parameters for simple systems." *Earthquake Engineering and Structural Dynamics*, 8(3), 197-217.
- Yang, X.S. (2010). "Engineering optimization: An introduction with metaheuristic applications." John Wiley & Sons, Inc., Hoboken, New Jersey, USA.
- Zuo, L., and Cui, W. (2013). "Dual-functional energy-harvesting and vibration control: Electromagnetic resonant shunt series tuned mass dampers." *Journal of Vibration and Acoustics*, ASME, 135(5), 051018-1-051018-9.